Universal robustness characteristic of weighted networks against cascading failure

Wen-Xu Wang* and Guanrong Chen†

Department of Electronic Engineering, City University of Hong Kong, Hong Kong SAR, People's Republic of China

(Received 22 May 2007; published 1 February 2008)

We investigate the cascading failure on weighted complex networks by adopting a local weighted flow redistribution rule, where the weight of an edge is $(k_i k_j)^\theta$ with k_i and k_j being the degrees of the nodes connected by the edge. Assume that a failed edge leads only to a redistribution of the flow passing through it to its neighboring edges. We found that the weighted complex network reaches the strongest robustness level when the weight parameter $\theta=1$, where the robustness is quantified by a transition from normal state to collapse. We determined that this is a universal phenomenon for all typical network models, such as small-world and scale-free networks. We then confirm by theoretical predictions this universal robustness characteristic observed in simulations. We furthermore explore the statistical characteristics of the avalanche size of a network, thus obtaining a power-law avalanche size distribution together with a tunable exponent by varying θ. Our findings have great generality for characterizing cascading-failure-induced disasters in nature.

DOI: 10.1103/PhysRevE.77.026101 PACS number(s): 89.75.Hc

The robustness characteristic of complex networks against attacks and random failures has drawn a great deal of attention in the past decade [1–4]. In particular, this issue is crucial for a large number of technological networks, on which modern human society very much relies. Such networks include power grids, information communication networks, and transportation networks, to name just a few. Evidence has demonstrated that in such a network, even though intentional attacks and random failures emerge very locally, the entire network can be affected, often resulting in global collapse. Typical examples are several blackouts in some countries [5] and Internet congestion [6,7]. These severe incidents have been attributed to cascading behaviors, and have been investigated quite intensively recently [3].

In the current studies of complex networks, several important properties shared by most networks have been discovered, subject to not only the topology but also the weights. It has been found that the small-world (SW) and scale-free (SF) properties are ubiquitous in nature and human society [1]. It is now known that the network structure plays a significant role in the dynamical process taking place on the network. Understanding this issue is regarded as one of the major objectives in the study of complex networks [2]. Therefore, it is natural and important to consider cascading failures on SW and SF networks in order to better understand and control various cascading-failure-induced disasters. For this purpose, many network models have been proposed and studied, such as the sandpile model [8–10], the global load-based cascading model (GLBCM) [11–17], and the fiber bundle model (FBM) [18–20]. Based on these models, some protection strategies have also been proposed [13,15,17,21]. However, the network weights have not been taken into consideration in these models, regardless of the facts that real networks display a large heterogeneity in the weights which have a strong correlation with the network topology [22]. In addition, the existing common weighted features play a significant role in a variety of dynamical processes [23–25]. Hence, there is a need for a modeling approach that can capture the coupling of cascading and weighted characteristics.

In this paper, we propose a cascading model with a local weighted flow redistribution rule (LWFRR) on weighted networks. The proposal is inspired by both GLBCM and FBM, in which the load redistribution or sharing (triggered by attacks or failures) and the finite capacities are regarded as two underlying mechanisms contributing to the cascading reactions. The LWFRR combines the cascading process and the weighted characteristics of the network. For two typical networks, i.e., the Barabási-Albert (BA) SF [26] and Newman-Watts (NW) SW networks [27], we found the strongest robustness level against cascading failures at a specific weighting strength. The robustness is quantified by the critical weighting threshold of edges, at which a phase transition occurs from normal state to collapse. Our theoretical analysis based on the mean-field theory confirms the numerical simulations. We also found tunable power-law distributions of avalanche sizes, which can generally reproduce the real observations.

Now, we briefly describe the cascading model under the LWFRR. We assume the weight (flow) of an edge ij to be $w_{ij}=(k_i k_j)^\theta$, where θ is a tunable weight parameter, governing the strength of the edge weight, and k_i and k_j are the degrees of nodes i and j, respectively. This assumption is supported by empirical evidence of real weighted networks [22]. Moreover, Ref. [28] shows that the betweenness of an edge has positive correlation with the product form of node degrees at both ends of the edge. In this sense, our assumption on the weights is in accordance with the previous load-based model but has practical convenience. Assume that the potential cascading failure is triggered by a small initial attack, e.g., cutting a single edge. The flow along the broken edge ij will be redistributed to the neighboring edges connecting to the ends of ij (see Fig. 1 for illustration). The additional flow ΔF_{im} received by edge im is proportional to its weight, i.e.,

*wenxuw@gmail.com
†gchen@ee.cityu.edu.hk

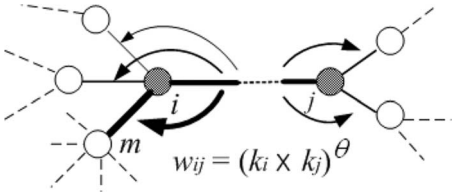

FIG. 1. Illustration of the LWFRR triggered by an edge-cut-based attack. Edge ij is broken and the flow along it is redistributed to the neighboring edges connecting to both ends of ij. Among these neighbor edges, the one with higher flow will receive higher shared flow from the broken edge.

$$\Delta F_{im} = F_{ij} \frac{w_{im}}{\sum_{a \in \Gamma_i} w_{ia} + \sum_{b \in \Gamma_j} w_{jb}}, \tag{1}$$

where Γ_i and Γ_j are the sets of neighboring nodes of i and j, respectively. If edge ij does not receive additional flows before being broken, $F_{ij}=w_{ij}$. Here, following previous models [13,14,17,20,21], each edge im has a weight threshold, which is the maximum flow that the edge can transmit. In manmade networks, the threshold is limited by cost. Thus, it is natural to assume that the threshold is proportional to its weight, i.e., Tw_{im}, where the constant $T>1$ is a threshold parameter. If

$$F_{im} + \Delta F_{im} > Tw_{im}, \tag{2}$$

then im will be broken and induce further redistribution of flow $F_{im}+\Delta F_{im}$ and potentially further edge breaking. After the cascading failure process stops, we calculate the avalanche size s, which is defined as the number of broken edges accumulated through the process.

The LWFRR can be explained by taking the scenario of information traffic on the Internet as an example. After congestion occurs on a transmission line, information flow is rerouted to bypass it, which leads to the flow increment of other lines. Since an edge of higher traffic flows has broader bandwidth for traffic transmission, i.e., an edge's threshold is proportional to its weight, it is reasonable to preferentially reroute traffic along those higher-capacity edges to maintain normal functioning of traffic and try to avoid further congestions. For simplicity, we assume that the additional flow received by an edge is proportional to its weight (flow). When a line receives extra flow, its total flow may exceed its bandwidth (threshold) and congestion occurs consequently. As a result, an avalanche of overloads emerges on the network. This data traffic redistribution may be global or local, depending on the network structure and rerouting protocols. In fact, global and local rerouting protocols both exist [16,20]. A very recent example is the submarine earthquake near Taiwan in December 2006; when a few important optical cables were broken, information transmissions were significantly delayed over many countries particularly in the Asia-Pacific region [7].

To explore the effect of a small initial attack on our cascading model, we cut only one edge ij initially and calculate s_{ij} (here s_{ij} denotes the avalanche size, i.e., the number of broken edges, induced by cutting ij) after the cascading process is over. To quantify the robustness of the whole network, we adopt the normalized avalanche size $S_N = \Sigma_{ij} s_{ij} / N_{\text{edge}}$, obtained via summation over all the avalanche sizes by cutting each edge initially at each time divided by the total number of edges N_{edge}.

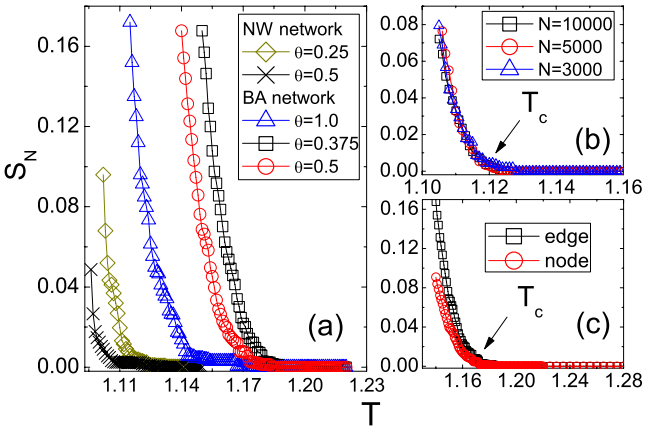

FIG. 2. (Color online) Normalized avalanche size S_N as a function of threshold T for (a) different values of θ on both BA and NW networks (network size 5000) and (b) different network sizes for BA networks. (c) Both the S_N of edges and nodes for BA networks. The phase transition points are the same. The average degree of BA networks is $\langle k \rangle = 4$. The coordination number of NW networks is 2 and the parameter $p=1.0$. Here, if all edges of a node is cut, the node fails. The avalanche size of node is the number of failed nodes normalized by the total number of nodes in the network.

Figure 2 shows S_N as a function of the threshold parameter T for BA and NW networks. BA and NW networks are constructed by the preferential attachment mechanism [26] and by randomly adding edges to a regular ring graph [27], respectively. A phase transition occurs at the critical threshold T_c, which can be used as a measure of the robustness of the network against cascading failure. When $T>T_c$, no cascading failure occurs and the system maintains its normal and efficient functioning; while for $T<T_c$, S_N suddenly increases from 0 and cascading failure emerges, causing the whole or part of the network to stop working. Hence T_c is the least value of protection strength to avoid cascading failure. Apparently, the lower the value of T_c, the stronger the robustness of the network against cascading failure.

Hereafter, we investigate the relationship between θ and the critical threshold T_c of BA and NW networks. As shown in Fig. 3, all these networks display the strongest robustness level at $\theta=1$ for all different average degrees. Here, we should briefly introduce a recent work of Korniss [29], in which $\theta=-1$ is found to be the optimum for synchronization in weighted networks, where the weight assignment of edges is the same as that in our weighted networks. However, in our study, $\theta=1$ is the optimum value for the weighted network against cascading failures, and the values of T_c at $\theta=-1$ are much higher than that at $\theta=1$ [30]. These different optimal values of θ results from the dynamical difference between cascading process and synchronization.

In order to understand this observed universal phenomenon, we provide some theoretical analysis. To avoid the emergence of cascading failure, the following condition should be satisfied [see (1) and (2)]:

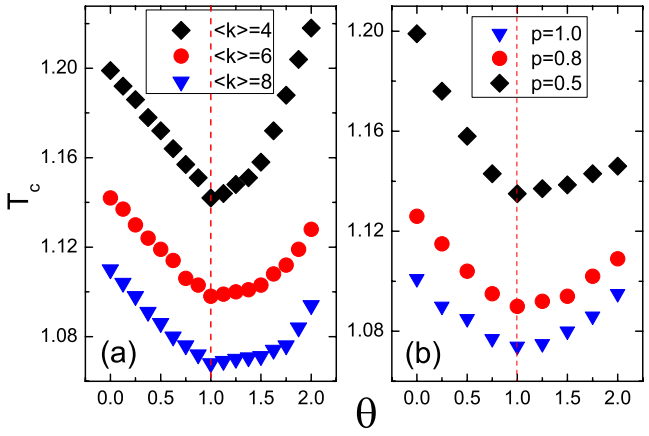

FIG. 3. (Color online) Robustness T_c as a function of θ for different average degrees $\langle k\rangle$ on BA networks and different p on NW networks. $p=1$ corresponds to a random network. $N=5000$, and each data point is averaged over ten different network realizations. For the BA model, $\langle k\rangle=2m$, where m is the number of edges attached to the existing nodes from the new node and $k_{\min}=m$. For the NW model, $\langle k\rangle=2(n_0+p)$, where n_0 is the coordinate number and p is the probability for each node to receive one edge.

$$\frac{(k_ik_j)^\theta(k_ik_m)^\theta}{\sum_{a\in\Gamma_i}(k_ik_a)^\theta+\sum_{b\in\Gamma_j}(k_jk_b)^\theta}+(k_ik_m)^\theta<T(k_ik_m)^\theta. \tag{3}$$

Here $\Sigma_{a\in\Gamma_i}(k_ik_a)^\theta=k_i^\theta\Sigma_{k'=k_{\min}}^{k_{\max}}k_iP(k'|k_i)k'^\theta$, where $P(k'|k_i)$ is the conditional probability that a node of k_i has a neighbor of k'. BA and NW networks have no degree-degree correlation; thus $P(k'|k_i)=k'P(k')/\langle k\rangle$. Hence, we have

$$\sum_{a\in\Gamma_i}(k_ik_a)^\theta=k_i^{\theta+1}\sum_{k'=k_{\min}}^{k_{\max}}\frac{k'^{\theta+1}P(k')}{\langle k\rangle}=\frac{k_i^{\theta+1}\langle k^{\theta+1}\rangle}{\langle k\rangle}. \tag{4}$$

Then Eq. (3) can be simplified as

$$\frac{\langle k\rangle}{\langle k^{\theta+1}\rangle}\frac{k_i^\theta k_j^\theta}{k_i^{1+\theta}+k_j^{1+\theta}}+1<T. \tag{5}$$

By noting that $k_i^{1+\theta}+k_j^{1+\theta}\geq 2(k_ik_j)^{(1+\theta)/2}$, we have

$$\frac{\langle k\rangle(k_ik_j)^{(\theta-1)/2}}{2\langle k^{\theta+1}\rangle}+1<T. \tag{6}$$

From the above inequality, the critical threshold T_c can be chosen by considering the ranges of $\theta<1$, $\theta=1$, and $\theta>1$, respectively:

$$T_c=\begin{cases}k_{\max}^{\theta-1}\langle k\rangle/(2\langle k^{\theta+1}\rangle)+1, & \theta>1,\\ \langle k\rangle/(2\langle k^2\rangle)+1, & \theta=1,\\ k_{\min}^{\theta-1}\langle k\rangle/(2\langle k^{\theta+1}\rangle)+1, & \theta<1,\end{cases} \tag{7}$$

where $k_{\min}$ and $k_{\max}$ are the minimum and maximum node degrees. To find the minimum value of T_c, we consider T_c-1 in the case of $\theta>1$ in Eq. (7):

$$\begin{aligned}T_c(\theta>1)-1&=\frac{k_{\max}^{\theta-1}\langle k\rangle}{2\langle k^{\theta+1}\rangle}=\frac{k_{\max}^{\theta-1}\langle k\rangle}{N}\\&=\frac{\langle k\rangle}{N}\\&>\frac{\langle k\rangle}{N}=\frac{\langle k\rangle}{2\langle k^2\rangle}.\end{aligned} \tag{8}$$

Hence, $T_c(\theta>1)>T_c(\theta=1)$. Similarly, we can get $T_c(\theta<1)>T_c(\theta=1)$. Apparently, the lowest value of T_c at $\theta=1$ indicates that the system possesses the universal strongest robustness, independent of the degree distribution of the network. Furthermore, one can notice that the result in Eq. (7) at $\theta=1$ is related with the critical infection rate of epidemic spreading in a susceptible-infected-susceptible model [31–33]. This relationship may indicate the similarity in dynamical behaviors of epidemic spreading and cascading failure.

There are two points of T_c that can be easily calculated by Eq. (7) without relying on simulations, i.e.,

$$T_c^{\mathrm{BA}}(\theta=0)=1/(2k_{\min})+1,$$

$$T_c^{\mathrm{MW}}(\theta=1)=1/(2\langle k\rangle)+1. \tag{9}$$

Here, $\langle k\rangle/\langle k^2\rangle\approx 1/\langle k\rangle$ for the NW network due to its homogeneous degree distribution. For the BA network with finite size, T_c at $\theta=1$ can be also calculated by integrations. The degree distribution of BA networks is $P(k)=2k_{\min}^2k^{-3}$ [26]. Hence $\langle k^2\rangle$ can be obtained by

$$\int_{k_{\min}}^{k_{\max}}P(k)k^2dk=2k_{\min}^2(\ln k_{\max}-\ln k_{\min}). \tag{10}$$

$k_{\max}$ can be calculated by $\int_{k_{\max}}^{\infty}P(k)dk=1/N$, which gives $k_{\max}=k_{\min}\sqrt{N}$, where N is the network size. Hence,

$$\langle k^2\rangle=2k_{\min}^2[\ln(k_{\min}\sqrt{N})-\ln k_{\min}]=k_{\min}^2\ln N. \tag{11}$$

Then we get

$$T_c^{\mathrm{BA}}(\theta=1)=1+\frac{\langle k\rangle}{2\langle k^2\rangle}=1+\frac{1}{k_{\min}\ln N}. \tag{12}$$

The comparison between simulation results and analytical predictions is shown in Figs. 4(a) and 4(b). In the case of $\theta=1$ for the BA network, the difference between simulation and analytical results is large, which mainly results from one approximation in the analytical predictions. For the BA network with finite size, the exponent of power-law degree distribution is higher than −3. Hence the use of $P(k)\sim k^{-3}$ leads to the difference in comparison.

Another prominent phenomenon empirically observed in the cascading failure process is the power-law avalanche size distribution. To explore the statistical features of the avalanche sizes, we continuously increase the flow along edges

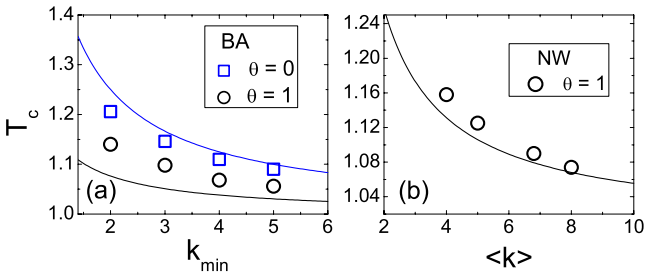

FIG. 4. (Color online) A comparison of analytical results and theoretical predictions on T_c vs $k_{\min}$ (θ=0 and θ=1) for BA networks and vs. $\langle k \rangle$ (θ=1) for NW networks. Data points are by simulations and curves are by theory.

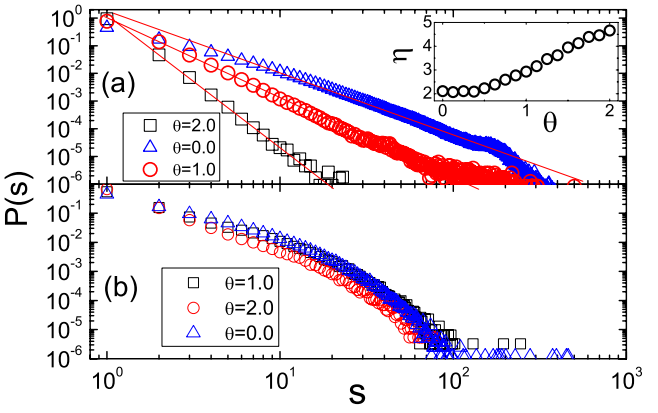

FIG. 5. (Color online) Distributions of the avalanche sizes for both (a) BA and (b) NW networks for different θ. The inset of (a) shows the exponent η of the power-law distribution, $P(s) \sim s^{-\eta}$, depending on θ. N=5000 and δ=0.01. The avalanche size is calculated as follows. At each time step, after the cascading process stops, record the number of broken edges as the avalanche size at this time step. Then recover all broken edges and set their flows to zero. At the next time step, add flow δ to randomly selected edges and repeat the cascading process. After the time step has lasted 10^8, we obtain the avalanche distribution $P(s)$ of the sizes recorded at each time step. If no cascading failures occur, s=0.

by a small constant δ, starting from an empty network. This process is essentially the same with the FBM and the sandpile model [9,20]. Here, the threshold of each edge is assumed to be its weight for simplicity. At any time step, add δ to one randomly selected edge. If the flow of the edge exceeds its threshold, the edge is broken and the flow will be redistributed according to the LWFRR. As shown in Fig. 5(a), for the BA model, the avalanche size displays a typical power-law distribution $P(s) \sim s^{-\eta}$, where η is a function of θ. For the NW model [Fig. 5(b)], $P(s)$ shows an exponential law, which implies that the homogeneous degree distribution of the NW may inhibit the emergence of a large area of avalanches. In previous work, η can only be tuned by the degree distribution exponent γ [9] or the geographic restriction [10]. In this sense, our model may shed some new light on the cascading failure mechanism.

In conclusion, we have investigated the cascading reaction behaviors on various weighted networks with respect to small edge-based initial attacks. We found that all studied weighted networks reach their strongest robustness level when the weight parameter equals 1. These results indicate the significant roles of weights in complex networks for designing protection strategies against cascading failures. In addition, the obtained tunable power-law distributions of the avalanche sizes demonstrate the validity and generality of our model for characterizing cascading reaction behaviors. Our work may have practical implications for controlling various cascading-failure-induced disasters in the real world.

We thank Dr. Jinhu Lu, Dr. Beom Jun Kim, Dr. Chengqing Li, and Wilson Thang for valuable suggestions. This work was supported by the NSFC-RGC under Grant No. N-CityU107/07 and NSFC under Grant No. 10635040.

[1] R. Albert and A.-L. Barabási, Rev. Mod. Phys. **74**, 47 (2002); S. N. Dorogovtsev and J. F. F. Mendes, Adv. Phys. **51**, 1079 (2002).
[2] M. E. J. Newman, SIAM Rev. **45**, 167 (2003).
[3] S. Boccaletti, V. Latora, Y. Moreno, M. Chavez, and D. U. Hwang, Phys. Rep. **424**, 175 (2006).
[4] R. Albert, H. Jeong, and A.-L. Barabàsi, Nature (London) **406**, 378 (2000); R. Cohen, K. Erez, D. ben-Avraham, and S. Havlin, Phys. Rev. Lett. **85**, 4626 (2000); D. S. Callaway, M. E. J. Newman, S. H. Strogatz, and D. J. Watts, *ibid.* **85**, 5468 (2000); S. N. Dorogovtsev and J. F. F. Mendes, *ibid.* **87**, 219801 (2001); L. K. Gallos, R. Cohen, P. Argyrakis, A. Bunde, and S. Havlin, *ibid.* **94**, 188701 (2005); P. Holme and B. J. Kim, Phys. Rev. E **65**, 066109 (2002).
[5] M. L. Sachtjen, B. A. Carreras, and V. E. Lynch, Phys. Rev. E **61**, 4877 (2000).
[6] V. Jacobson, Comput. Commun. Rev. **18**, 314 (1988); R. Guimerà, A. Arenas, A. Diaz-Guilera, and F. Giralt, Phys. Rev. E **66**, 026704 (2002).
[7] More information can be seen in http://www.ofta.gov.hk/en/press-rel/2006/Dec-2006_r4.html
[8] P. Bak, C. Tang, and K. Wiesenfeld, Phys. Rev. Lett. **59**, 381 (1987); Phys. Rev. A **38**, 364 (1988).
[9] K.-I. Goh, D. S. Lee, B. Kahng, and D. Kim, Phys. Rev. Lett. **91**, 148701 (2003).
[10] L. Huang, L. Yang, and K. Yang, Phys. Rev. E **73**, 036102 (2006).
[11] A. E. Motter and Y.-C. Lai, Phys. Rev. E **66**, 065102(R) (2002).
[12] Y. Moreno, R. Pastor-Satorras, A. Vázquez, and A. Vespignani, Europhys. Lett. **62**, 292 (2003).
[13] A. E. Motter, Phys. Rev. Lett. **93**, 098701 (2004).
[14] L. Zhao, K. Park, and Y.-C. Lai, Phys. Rev. E **70**, 035101(R) (2004).
[15] L. Zhao, K. Park, Y. C. Lai, and N. Ye, Phys. Rev. E **72**, 025104(R) (2005).

[16] P. Crucitti, V. Latora, and M. Marchiori, Phys. Rev. E **69**, 045104(R) (2004).
[17] M. Schäfer, J. Scholz, and M. Greiner, Phys. Rev. Lett. **96**, 108701 (2006).
[18] Y. Moreno, J. B. Gómez, and A. F. Pacheco, Europhys. Lett. **58**, 630 (2002).
[19] B. J. Kim, Europhys. Lett. **66**, 819 (2004).
[20] D.-H. Kim, B. J. Kim, and H. Jeong, Phys. Rev. Lett. **94**, 025501 (2005).
[21] B. Wang and B. J. Kim, Europhys. Lett. **78**, 48001 (2007).
[22] A. Barrat, M. Barthélemy, R. Pastor-Satorras, and A. Vespignani, Proc. Natl. Acad. Sci. U.S.A. **101**, 3747 (2004); P. J. Macdonald, E. Almaas, and A.-L. Barabási, Europhys. Lett. **72**, 308 (2005).
[23] A. E. Motter, C. Zhou, and J. Kurths, Phys. Rev. E **71**, 016116 (2005).
[24] C. Zhou, A. E. Motter, and J. Kurths, Phys. Rev. Lett. **96**, 034101 (2006).
[25] Z. Zhang, S. Zhou, L. Chen, J. Guan, L. Fang, and Y. Zhang, Eur. Phys. J. B **59**, 99 (2007).
[26] A.-L. Barabási and R. Albert, Science **286**, 509 (1999).
[27] M. E. J. Newman and D. J. Watts, Phys. Rev. E **60**, 7332 (1999).
[28] P. Holme, B. J. Kim, C. N. Yoon, and S. K. Han, Phys. Rev. E **65**, 056109 (2002).
[29] G. Korniss, Phys. Rev. E **75**, 051121 (2007).
[30] We have checked that for BA networks, when $\theta=-1$, $T_c^{\langle k\rangle=4}=1.34$, $T_c^{\langle k\rangle=6}=1.27$, and $T_c^{\langle k\rangle=8}=1.17$, which indicates that T_c at $\theta=-1$ is much larger than that at $\theta=1$.
[31] R. Pastor-Satorras and A. Vespignani, Phys. Rev. Lett. **86**, 3200 (2001).
[32] M. Bogunä, R. Pastor-Satorras, and A. Vespignani, Phys. Rev. Lett. **90**, 028701 (2003).
[33] M. Barthélemy, A. Barrat, R. Pastor-Satorras, and A. Vespignani, Phys. Rev. Lett. **92**, 178701 (2004).